

---

# TPC: Transformation-Specific Smoothing for Point Cloud Models

---

Wenda Chu<sup>1</sup> Linyi Li<sup>2</sup> Bo Li<sup>2</sup>

## Abstract

Point cloud models with neural network architectures have achieved great success and been widely used in safety-critical applications, such as Lidar-based recognition systems in autonomous vehicles. However, such models are shown vulnerable against adversarial attacks which aim to apply stealthy semantic transformations such as rotation and tapering to mislead model predictions. In this paper, we propose a transformation-specific smoothing framework TPC, which provides *tight* and *scalable* robustness guarantees for point cloud models against semantic transformation attacks. We first categorize common 3D transformations into three categories: additive (e.g., shearing), composable (e.g., rotation), and indirectly composable (e.g., tapering), and we present generic robustness certification strategies for all categories respectively. We then specify unique certification protocols for a range of specific semantic transformations and their compositions. Extensive experiments on several common 3D transformations show that TPC significantly outperforms the state of the art. For example, our framework boosts the certified accuracy against twisting transformation along  $z$ -axis (within  $\pm 20^\circ$ ) from 20.3% to 88.8%.

## 1. Introduction

Deep neural networks that take point clouds data as inputs (point cloud models) are widely used in computer vision (Qi et al., 2017; Wang et al., 2019; Zhou & Tuzel, 2018) and autonomous driving (Li, 2017; Chen et al., 2017; 2020). For instance, modern autonomous driving systems are equipped with LiDAR sensors that generate point cloud inputs to feed into point cloud models (Cao et al., 2019). Despite their successes, point cloud models are shown vul-

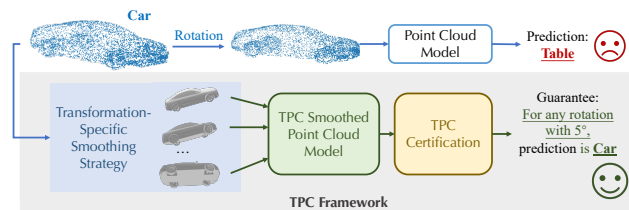


Figure 1. Overview of TPC framework. TPC includes smoothing and certification strategies to provide certified robustness for point cloud models against semantic transformations. Besides rotation as shown in figure, TPC provides strong robustness certification for a wide range of other semantic transformations.

nerable to adversarial attacks that mislead the model’s prediction by adding stealthy perturbations to point coordinates or applying semantic transformations (e.g., rotation, shearing, tapering) (Cao et al., 2019; Xiang et al., 2019; Xiao et al., 2019; Fang et al., 2021). Specifically, semantic transformation based attacks can be easily operated on point cloud models by simply manipulating sensor positions or orientations (Cao et al., 2019; 2021). These attacks may lead to severe consequences such as forcing an autonomous driving vehicle to steer towards the cliff (Pei et al., 2017). A wide range of empirical defenses against these attacks have been studied (Zhu et al., 2017; Aoki et al., 2019; Sun et al., 2020), while defenses with robustness guarantees is less explored (Lorenz et al., 2021) and provides loose and less scalable certification.

In this paper, we propose a transformation-specific smoothing framework TPC which provides *tight* and *scalable* robustness guarantees for point cloud models against a wide range of semantic transformation attacks. We first categorize common semantic transformations into three categories: additive (e.g., shearing), composable (e.g., rotation), and indirectly composable (e.g., tapering). For each category, our framework proposes novel *smoothing* and *robustness certification* strategies. With TPC, for each common semantic transformation or their composition, we prove the corresponding robustness conditions that yield efficient and tight robustness certification.

For example, regarding general rotation based attacks, we first prove that it is a type of *composable* transformations; we then propose corresponding smoothing strategy and certify the robustness of the smoothed model with a novel sampling-based algorithm which is shown to have sound and

---

<sup>1</sup>Institute for Interdisciplinary Information Sciences, Tsinghua University, Beijing, P. R. China <sup>2</sup>University of Illinois Urbana Champaign, Illinois, USA. Correspondence to: Linyi Li <linyi2@illinois.edu>.

tight input-dependent sampling error bound. TPC achieves 69.2% certified robust accuracy for any rotation within  $10^\circ$ . To the best of our knowledge, no prior work can provide robustness certification for rotations within such large angles.

In addition to our theoretical analysis for the certification against different types of semantic transformations, we conduct extensive experiments to evaluate TPC. Compared with existing baselines, our TPC achieves *substantially* higher certified robust accuracy than existing baselines. For example, for any twisting along  $z$ -axis within  $\pm 20^\circ$ , we improve the certified accuracy from 20.3% (Lorenz et al., 2021) to 83.8%. Furthermore, compared with prior works, we show that TPC can: (1) certify a more general class of semantic transformations; (2) certify large-size point clouds; and (3) certify under large perturbation magnitudes. We also show that TPC can certify the robustness for multiple tasks on 3D point clouds, including classification and part segmentation.

We illustrate our TPC framework in Figure 1, and we summarize the main technical **contributions** as follows.

- We propose a general robustness certification framework TPC for point cloud models. We categorize common semantic transformations of point clouds into three categories: additive, composable, and indirectly composable, and provide general smoothing and certification strategies for each.
- We concretize our framework TPC to provide transformation-specific smoothing and certification for various realistic common semantic transformations for point clouds, including rotation, shearing, twisting, tapering as well as their compositions.
- We conduct extensive experiments and show that TPC (1) achieves significantly higher certified robust accuracy than baselines, (2) provides certification for large-size point clouds and large perturbation magnitudes, (3) provides efficient and effective certification for different tasks such as classification and part segmentation.

## Related Work

**Certified Robustness of Deep Neural Networks.** To mitigate the threats of adversarial attacks on deep neural networks (Szegedy et al., 2013; Tramer et al., 2020; Eykholt et al., 2018; Qiu et al., 2020; Li et al., 2020a; Zhang et al., 2022; Li et al., 2021a; Xiao et al., 2018), efforts have been made toward certifying and improving the certified robustness of DNNs (Cohen et al., 2019a; Li et al., 2020b; 2019). Existing works mainly focus on image classification models against  $\ell_p$  bounded perturbations. For such threat model, the robustness certification can be roughly divided into two types: deterministic and probabilistic, where deterministic methods are mainly based on feasible region

relaxation (Wong & Kolter, 2018; Weng et al., 2018; Zhang et al., 2018), abstract interpretation (Mirman et al., 2018; Singh et al., 2019), or Lipschitz bounds (Tsuzuku et al., 2018; Zhang et al., 2021); and probabilistic methods provide certification that holds with high probability and they are mainly based on randomized smoothing (Cohen et al., 2019b; Yang et al., 2020). Along with the certification methods, there are several robust training methods that aim to train DNNs to be more certifiably robust (Wong et al., 2018; Li et al., 2019; Salman et al., 2019).

**Semantic Transformation Attacks and Certified Robustness on Point Cloud Models.** Our TPC aims to generalize the model robustness certification to point cloud models against a more generic family of practical attacks – semantic transformation attacks. The semantic transformation attacks have been shown feasible for both image classification models and point cloud models (Hendrycks & Dietterich, 2018; Cao et al., 2019; Xiang et al., 2019), and certified robustness against such attacks are mainly studied for 2D image classification models (Balunović et al., 2019; Fischer et al., 2020; Li et al., 2021b). For point cloud models, some work considers point *addition* and *removal* attacks (Xiang et al., 2019), and provides robustness certification against such attacks (Liu et al., 2021). However, for semantic transformation attacks, to the best of our knowledge, the only work that is able to provide robustness certification against them is DeepG3D (Lorenz et al., 2021), which is based on linear bound relaxations. In this work, we derive novel randomized smoothing techniques on point clouds models to provide robustness certification against semantic transformations. In Section 5, we conduct extensive experiments to show that our framework is more general and provides significantly higher certified robust accuracy than DeepG3D under different settings.

## 2. Semantic Transformation Attacks on Point Cloud Models

We denote the space of point cloud inputs as  $\mathcal{X} = \mathbb{R}^{N \times 3}$  where  $N$  is the number of points the point cloud has. A point cloud with  $N$  points is denoted by  $x = \{p_i\}_{i=1}^N$  with  $p_i \in \mathbb{R}^3$ . Unless otherwise noted, we assume all point cloud inputs are normalized to be within a unit ball, i.e.,  $\|p_i\|_2 \leq 1$ . A classification task is defined with a set of labels  $\mathcal{Y} = \{1, \dots, C\}$  and a classifier is defined by a deterministic function  $h : \mathcal{X} \rightarrow \mathcal{Y}$ .

### 2.1. Semantic Transformations

Semantic transformations on point cloud models are defined as functions  $\phi : \mathcal{X} \times \mathcal{Z} \rightarrow \mathcal{X}$  where  $\mathcal{Z}$  is the parameter space for transformations. The semantic transformations discussed in this paper may change the three dimensional coordinate of each point (usually in a pointwise manner),

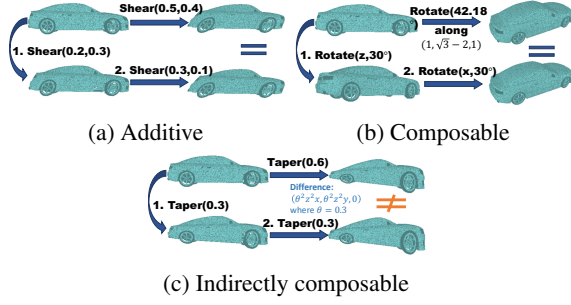


Figure 2. Illustration of different types of transformations. (a) additive transformations (e.g., shearing), (b) composable transformations (e.g., rotation) and (c) indirectly composable transformations (e.g., tapering).

but do not increase or decrease the number of points. In Section 3, we will further categorize different semantic transformations based on their intrinsic properties.

## 2.2. Threat Model and Certification Goal

We consider semantic transformation attacks that an adversary can apply arbitrary semantic transformations to the point cloud data according to a parameter  $z \in \mathcal{Z}$ . The adversary then perform evasion attacks to a classifier  $h$  with the transformed point cloud  $\phi(x, z)$ . The attack is successful if  $h$  predicts different labels on  $x$  and  $\phi(x, z)$ <sup>1</sup>.

The main goal of this paper is to certify the robustness of point cloud classifiers against all semantic attacks within a certain transformation parameter space. Formally, our **certification goal** is to find a subset  $\mathcal{Z}_{\text{robust}} \subseteq \mathcal{Z}$  for a classifier  $h : \mathcal{X} \rightarrow \mathcal{Y}$ , such that

$$h(x) = h(\phi(x, z)), \forall z \in \mathcal{Z}_{\text{robust}} \quad (1)$$

## 3. Transformation Specific Smoothing for Point Cloud Models

In this section, we first introduce the proposed randomized smoothing techniques for general semantic transformations. Next we categorize the semantic transformations into three types: composable, additive and indirectly composable transformations. We then derive the smoothing based certification strategies for each type.

### 3.1. Transformation Specific Smoothed Classifier

We apply transformation specific smoothing to an arbitrary base classifier  $h : \mathcal{X} \rightarrow \mathcal{Y}$  to construct a smoothed classifier. Specifically, the smoothed classifier  $g$  predicts the class with the highest conditional probability when the input  $x$  is perturbed by some random transformations.

**Definition 1** (Transformation Specific Smoothed Classifier).

<sup>1</sup>Without loss of generality, we consider untargeted attacks here and the targeted attack can be derived similarly

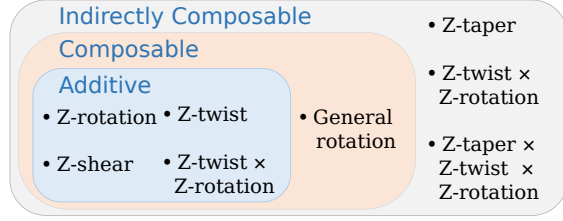


Figure 3. Taxonomy of common 3D semantic transformations for point clouds.

Let  $\phi : \mathcal{X} \times \mathcal{Z} \rightarrow \mathcal{X}$  be a semantic transformation. Let  $\epsilon$  be a random variable in the parameter space  $\mathcal{Z}$ . Suppose we have a base classifier that learns a conditional probability distribution,  $h(x) = \arg \max_{y \in \mathcal{Y}} p(y|x)$ . Applying transformation specific smoothing to the base classifier  $h$  yields a smoothed classifier  $g : \mathcal{X} \rightarrow \mathcal{Z}$ , which predicts

$$g(x; \epsilon) = \arg \max_{y \in \mathcal{Y}} q(y|x, \epsilon) = \arg \max_{y \in \mathcal{Y}} \mathbb{E}_{\epsilon} (p(y|\phi(x, \epsilon))) \quad (2)$$

We recall the theorem proved by (Li et al., 2021b) in Appendix A.1, which provides a generic certification bound for transformation specific smoothed classifier based on the Neyman Pearson Lemma.

Next we will categorize the semantic transformations into different categories based on their intrinsic properties as shown in Figure 3, and we will then discuss the certification principles for each specific category.

### 3.2. Composable Transformations

A set of semantic transformations is called composable if it is closed under composition.

**Definition 2.** A set of semantic transformations defined by  $\phi : \mathcal{X} \times \mathcal{Z} \rightarrow \mathcal{X}$  is called **composable** if for any  $\alpha \in \mathcal{Z}$  there exists an injective and continuously differentiable function  $\gamma_{\alpha} : \mathcal{Z} \rightarrow \mathcal{Z}$  with non-vanishing Jacobian, such that

$$\phi(\phi(x, \alpha), \beta) = \phi(x, \gamma_{\alpha}(\beta)), \forall x \in \mathcal{X}, \beta \in \mathcal{Z} \quad (3)$$

Common semantic transformations for Point cloud data that are composable include: rotation, shearing along a fixed axis and twisting along a fixed axis. For example, according to Euler’s rotation theorem, we can always find another rotation  $\gamma_{\alpha}(\beta) \in \mathcal{Z}$  for any two rotations  $\alpha, \beta \in \mathcal{Z}$ . Therefore, rotations belong to the composable transformations as shown in Figure 2 (b).

In general, composable transformations can be certified against by Theorem 5 stated in Appendix A.1. For a classifier  $g(x; \epsilon_0)$  smoothed by the composable transformation, we can simply replace the random variable  $\epsilon_1$  by  $\gamma_{\alpha}(\epsilon)$  in Theorem 5 to derive a robustness certification condition. However, some composable transformations with complicated  $\gamma_{\alpha}(\beta)$  function result in intractable distribution for  $\epsilon_1$ , causing difficulties for the certification. Therefore, we focus

on a subset of composable transformations, called *additive transformations*, for which it is straight-forward to certify by applying Theorem 5.

### 3.3. Additive Transformations

We are particularly interested in a subset of composable transformations that the function  $\gamma_\alpha : \mathcal{Z} \rightarrow \mathcal{Z}$  defined in Definition 2 satisfies  $\gamma_\alpha(\beta) = \alpha + \beta$  as shown in Figure 2 (a) where the one step rotation above is equivalent to the two step transformations below.

**Definition 3.** A set of semantic transformations  $\phi : \mathcal{X} \times \mathcal{Z} \rightarrow \mathcal{X}$  is called **additive** if

$$\phi(\phi(x, \alpha), \beta) = \phi(x, \alpha + \beta), \forall x \in \mathcal{X}, \alpha, \beta \in \mathcal{Z}. \quad (4)$$

An additive transformation must be composable, but the reverse direction does not hold. For instance, the set of general rotations from the SO(3) group is composable, but not additive. Rotating  $10^\circ$  along x axis first and then  $10^\circ$  along y axis does not equal to rotating  $20^\circ$  along the xy axis. Thus, general rotations cannot be categorized as an additive transformation. However, rotating along any fixed axis is additive. Based on this observation, we discuss z-rotation (i.e., rotation along z axis) and general rotations separately in Section 4.

All additive transformations can be certified following the same protocol derived from Theorem 5. We omit Corollary 3 for certified robustness against additive transformation in Appendix A.1.

### 3.4. Indirectly Composable Transformations

As shown in Section 3.2, composable transformations can be certified following Theorem 5. However, some semantic transformations of point clouds do not have such closure property under composition and thus do not fall in this category as shown in Figure 2 (c). For example, the tapering transformation which we will discuss in Section 4 is not composable and cannot be certified directly using Theorem 5. This kind of transformations are therefore categorized as a more general class called indirectly composable transformations.

**Definition 4.** A set of transformations  $\phi : \mathcal{X} \times \mathcal{Z}_\phi \rightarrow \mathcal{X}$  is **indirectly composable** if there is a set of composable transformations  $\psi : \mathcal{X} \times \mathcal{Z}_\psi \rightarrow \mathcal{X}$ , such that for any  $x \in \mathcal{X}$ , there exists a function  $\delta_x : \mathcal{Z}_\phi \times \mathcal{Z}_\phi \rightarrow \mathcal{Z}_\psi$  with

$$\phi(x, \alpha) = \psi(\phi(x, \beta), \delta_x(\alpha, \beta)), \forall \alpha, \beta \in \mathcal{Z}_\phi. \quad (5)$$

This definition involves more kinds of transformations, since we can choose the transformation  $\psi$  as  $\psi(x, \delta) = x + \delta$  and let  $\delta_x(\alpha, \beta) = \phi(x, \alpha) - \phi(x, \beta)$ . This specific assignment of  $\psi$  leads to a useful theorem (Li et al., 2021b) in Appendix A.2, which we use to certify against some more complicated transformations, such as tapering in Section 4.

The theorem states that the overall robustness can be guaranteed if we draw multiple samples within the parameter space and certify the neighboring distribution of each sampled parameter separately.

## 4. Certifying Point Cloud Models against Specific Semantic Transformations

In this section, we certify the point cloud models against several specific semantic transformations that are commonly seen for point cloud data, including rotation, shearing, twisting and tapering. We do not analyze scaling and translation, since the point cloud models are usually inherently invariant to them due to the standard pre-processing pipeline (Qi et al., 2017). For each transformation, we specify a corresponding certification protocol based on the categorization they belong to introduced in Section 3.

### 4.1. Rotation, Shearing and Twisting along a Fixed Axis

Rotation, shearing and twisting are all common 3D transformations that are performed pointwisely on point clouds. Without loss of generality, we consider performing these transformations along the z-axis.

Specifically, we define **z-shear** transformation as  $\phi_{Sz} : \mathcal{X} \times \mathcal{Z} \rightarrow \mathcal{X}$  where  $\mathcal{X} = \mathbb{R}^{N \times 3}$  is the space of the point clouds with  $N$  points and  $\mathcal{Z} = \mathbb{R}^2$  is the parameter space. For any  $z = (\theta_1, \theta_2)$ , z-shear acting on a point cloud  $x \in \mathcal{X}$  with  $x = \{p_i\}_{i=1}^N$  yields  $(p_i = (x_i, y_i, z_i)^T)$

$$\phi_{Sz}(p_i, z) = (x_i + \theta_1 z_i, y_i + \theta_2 z_i, z_i). \quad (6)$$

**Z-twist** transformation  $\phi_{Tz} : \mathcal{X} \times \mathcal{Z} \rightarrow \mathcal{X}$  is defined similarly but with parameter space  $\mathcal{Z} = \mathbb{R}$ . For any  $\theta \in \mathcal{Z}$  and  $p_i = (x_i, y_i, z_i)^T$ ,

$$\phi_{Tz}(p_i, \theta) = \begin{pmatrix} x_i \cos(\theta z_i) - y_i \sin(\theta z_i) \\ x_i \sin(\theta z_i) + y_i \cos(\theta z_i) \\ z_i \end{pmatrix} \quad (7)$$

Note that z-rotation, z-shear and z-twist are all *additive* transformations. Hence, we present the following corollary based on Corollary 3, which certifies the robustness of point clouds models with bounded  $\ell_2$  norm for the transformation parameters.

**Corollary 1.** Suppose a classifier  $g : \mathcal{X} \rightarrow \mathcal{Y}$  is smoothed by a transformation  $\phi : \mathcal{X} \times \mathcal{Z} \rightarrow \mathcal{X}$  with  $\epsilon \sim \mathcal{N}(0, \sigma^2 \mathbb{1}_d)$ . Assume its class probability satisfies Equation (22). If the transformation is z-rotation, z-shear or z-twist ( $\phi = \phi_{Sz}, \phi_{Tz}$  or  $\phi_{Rot-z}$ ), then it is guaranteed that  $g(\phi(x, \alpha); \epsilon) = g(x; \epsilon)$ , if the following condition holds:

$$\|\alpha\|_2 \leq \frac{\sigma}{2} \left( \Phi^{-1}(p_A) - \Phi^{-1}(p_B) \right), \alpha \in \mathcal{Z} \quad (8)$$

## 4.2. Tapering along a Fixed Axis

Tapering a point keeps the coordinate of a specific axis  $k$ , but scales the coordinates of other axes proportional to  $k$ 's coordinate. For clarity, we define **z-taper** transformation  $\phi_{TP} : \mathcal{X} \times \mathcal{Z} \rightarrow \mathcal{X}$  as tapering along the z-axis, with its parameter space defined by  $\mathcal{Z} = \mathbb{R}$ . For any point cloud  $x = \{p_i\}_{i=1}^N \in \mathcal{X}$  ( $p_i = (x_i, y_i, z_i)$ ) and for any  $\theta \in \mathcal{Z}$ ,

$$\phi_{TP}(p_i, \theta) = (x_i(1 + \theta z_i), y_i(1 + \theta z_i), z_i). \quad (9)$$

However, z-taper is not a composable transformation, since the composition of two z-taper transformations contains terms with  $z_i^2$  component. We therefore propose a specific certification protocol for z-taper based on Theorem 6. To achieve this goal, we specify a sampling strategy in the parameter space  $\mathcal{Z}$  and bound the interpolation error (Equation (29)) of the sampled z-taper transformations.

**Theorem 1.** *Let  $\phi_{TP} : \mathcal{X} \times \mathbb{R} \rightarrow \mathcal{X}$  be a z-taper transformation. Let  $g : \mathcal{X} \rightarrow \mathcal{Y}$  be a  $\epsilon$ -smoothed classifier with random noises  $\epsilon \sim \mathcal{N}(0, \sigma^2 \mathbb{1}_{3 \times N})$ , which predicts  $g(x; \epsilon) = \arg \max_y q(y|x; \epsilon) = \arg \max_y \mathbb{E}_\epsilon p(y|x + \epsilon)$ . Let  $\{\theta_j\}_{j=0}^M$  be a set of transformation parameters and  $\theta_j = (\frac{2j}{M} - 1)R$ . Suppose for any  $i$ ,*

$$q(y_A | \phi_{TP}(x, \theta_j); \epsilon) \geq p_A^{(j)} > p_B^{(j)} \geq \max_{y \neq y_A} q(y | \phi_{TP}(x, \theta_j); \epsilon) \quad (10)$$

*Then it is guaranteed that  $\forall \theta \in [-R, R]$ :  $y_A = \arg \max_y q(y | \phi_{TP}(x, \theta); \epsilon)$  if for all  $j = 1, \dots, M$ ,*

$$\frac{\sigma}{2} \left( \Phi^{-1} \left( p_A^{(j)} \right) - \Phi^{-1} \left( p_B^{(j)} \right) \right) \geq \frac{R\sqrt{N}}{2M} \quad (11)$$

Detailed proof for Theorem 1 can be found in Appendix B.1

## 4.3. General Rotation

Rotation is the one of the most common transformations for point cloud data. Therefore, we hope the classifier is robust not only against rotation attacks along a fixed axis, but also those along arbitrary axes. In this section, we first define general rotation and show its universality for rotations as well as their composition; and then provide a concrete certification protocol for smoothing and certifying the robustness against it.

We define **general rotation** transformations as  $\phi_R : \mathcal{X} \times \mathcal{Z} \rightarrow \mathcal{X}$  where  $\mathcal{Z} = S^2 \times \mathbb{R}^+$  is the parameter space of rotations. For a rotation  $z \in \mathcal{Z}$ , its rotation axis is defined by a unit vector  $k \in S^2$  and its rotation angle is  $\theta \in \mathbb{R}^+$ . For any 3D point  $p_i \in \mathbb{R}^3$ ,

$$\phi_R(p_i, z) = \text{Rot}(k, \theta)p_i, \quad z = (k, \theta). \quad (12)$$

where  $\text{Rot}(k, \theta)$  is the rotation matrix that rotates by  $\theta$  along axis  $k$ . General rotations are *composable* transformations since the composition of any two 3D rotations can be expressed by another 3D rotation.

However, certifying against the general rotation is more challenging, since the general rotation is not additive and the expression of their composition is extremely complicated. In particular, if we smooth a base classifier with a random variable  $\epsilon_0$ , a semantic attack with parameter  $\alpha \in \mathcal{Z}$  results in  $\phi_R(\phi_R(x, \alpha), \epsilon_0) = \gamma_\alpha(\epsilon_0)$ , which is a bizarre distribution in the parameter space. Therefore, we cannot directly apply Theorem 5 to certify general rotation.

On the other hand, as Theorem 6 shows, if we uniformly sample many parameters in a subspace of  $\mathcal{Z} = S^2 \times \mathbb{R}^+$  and certify robustness in the neighborhood of each sample, we are able to certify a large and continuous subspace  $\mathcal{Z}_{\text{robust}} \subseteq \mathcal{Z}$ . As a result, we propose a sampling based certification strategy, together with a tight bound for interpolation error between general rotation transformations, which we summarize in the following theorem.

**Theorem 2.** *Let  $\phi_R : \mathcal{X} \times \mathcal{Z} \rightarrow \mathcal{X}$  be a general rotation transformation. Let  $g : \mathcal{X} \rightarrow \mathcal{Y}$  be a classifier smoothed by random noises  $\epsilon \sim \mathcal{N}(0, \sigma^2 \mathbb{1}_{3 \times N})$ , which predicts  $g(x; \epsilon) = \arg \max_y q(y|x; \epsilon) = \arg \max_y \mathbb{E}(p(y|x + \epsilon))$ . Let  $\{z_j\}_{j=1}^M$  be a set of transformation parameters with  $z_j = (k_j, \theta_j)$ ,  $k_j \in S^2$ ,  $\theta_j \in \mathbb{R}^+$  such that*

$$\forall k \in S^2, \theta \in [0, R], \exists k, \langle k, k_j \rangle \leq \epsilon, |\theta - \theta_j| \leq \delta \quad (13)$$

*Suppose for any  $j$ , the smoothed classifier  $g$  has class probabilities that satisfy*

$$q(y_A | \phi_R(x, z_j); \epsilon) \geq p_A^{(j)} > p_B^{(j)} \geq \max_{y \neq y_A} q(y | \phi_R(x, z_j); \epsilon). \quad (14)$$

*Then it is guaranteed that for any  $z$  with rotation angle  $\theta < R$ :  $y_A = \arg \max_y q(y | \phi_R(x, z); \epsilon)$  if  $\forall j$ ,*

$$\frac{\sigma}{2} \left( \Phi^{-1} \left( p_A^{(j)} \right) - \Phi^{-1} \left( p_B^{(j)} \right) \right) \geq \pi \sqrt{\frac{\delta^2}{4} + \frac{\epsilon^2 R^2}{8}} \|x\|_2. \quad (15)$$

We present a proof sketch here and leave the details in Appendix B.2. Notice that the interpolation error between two transformations on a point cloud  $x = \{p_i\}_{i=1}^N$  can be calculated by  $\|\phi(x, z_j) - \phi(x, z)\|_2 = \|\phi(x, z') - x\|_2 \leq \theta' (\sum_i^N \|p_i\|_2^2)^{1/2}$ , where  $z' = (k', \theta')$  is the composition of the rotation with parameter  $z$  and the reverse rotation  $z_j^{-1}$ . Combined with the generic theorem for indirectly composable transformations (Theorem 6), bounding  $\theta'$  using Equation (13) yields Theorem 2.

## 4.4. Compositions of Different Transformations

In addition to certifying against a single transformation, we also provide certification protocols for composite transformations, including z-twist  $\circ$  z-rotation, z-taper  $\circ$  z-rotation and z-twist  $\circ$  z-taper  $\circ$  z-rotation.

Notice that z-twist  $\circ$  z-rotation is an additive function:

$$\begin{aligned} \phi_{Tz}(\phi_{\text{Rot}-z}(\phi_{Tz}(\phi_{\text{Rot}-z}(x, \theta_1), \alpha_1), \theta_2), \alpha_2) \\ = \phi_{Tz}(\phi_{\text{Rot}-z}(x, \theta_1 + \theta_2), \alpha_1 + \alpha_2). \end{aligned} \quad (16)$$

Therefore, we directly apply Corollary 3 in Appendix A.1 to certify z-twist  $\circ$  z-rotation transformation. The concrete corollary is stated as below.

**Corollary 2.** *Suppose a classifier  $g : \mathcal{X} \rightarrow \mathcal{Y}$  is smoothed by random transformations z-twist  $\circ$  z-rotation  $\phi : \mathcal{X} \times \mathcal{Z} \rightarrow \mathcal{X}$  where the parameter space  $\mathcal{Z} = \mathcal{Z}_{Twist} \times \mathcal{Z}_{Rot-z} = \mathbb{R}^2$ . The random variable for smoothing is  $\epsilon \sim \mathcal{N}(0, \text{diag}(\sigma_1^2, \sigma_2^2))$ . If the class probability of  $g$  satisfies Equation (22), then it is guaranteed that  $g(\phi(x, \alpha); \epsilon) = g(x; \epsilon)$  for all  $(\alpha_1, \alpha_2) \in \mathcal{Z}$ , if the following condition holds:*

$$\sqrt{\left(\frac{\alpha_1}{\sigma_1}\right)^2 + \left(\frac{\alpha_2}{\sigma_2}\right)^2} \leq \frac{\sigma}{2} \left( \Phi^{-1}(p_A) - \Phi^{-1}(p_B) \right). \quad (17)$$

Another composite transformation z-taper  $\circ$  z-rotation first rotates the point cloud along z-axis, and then taper along z-axis. As z-taper is not composable with itself, this composite transformation is also not composable. Similar to z-taper, we certify the composite transformation z-taper  $\circ$  z-rotation by upper-bounding the interpolation error in Equation (29).

**Theorem 3.** *We denote z-taper  $\circ$  z-rotation by  $\phi : \mathcal{X} \times \mathcal{Z} \rightarrow \mathcal{X}$ ,  $\phi = \phi_{TP} \circ \phi_{Rot-z}$  with a parameter space of  $\mathcal{Z} = \mathcal{Z}_{TP} \times \mathcal{Z}_{Rot-z} = \mathbb{R}^2$ . Let  $g : \mathcal{X} \rightarrow \mathcal{Y}$  be a classifier smoothed by random noises  $\epsilon \sim \mathcal{N}(0, \sigma^2 \mathbb{1}_{3 \times N})$ .*

*For a subspace in the parameter space,  $S = [-\varphi, \varphi] \times [-\theta, \theta] \subseteq \mathcal{Z}$ , we uniformly sample  $\varphi\theta M^2$  parameters  $\{z_{jk}\}$  in  $S$ . That is,  $z_{jk} = (\varphi_j, \theta_k)$  where  $\varphi_j = \frac{2j}{M} - \varphi$  and  $\theta_k = \frac{2k}{M} - \theta$ . Suppose for any  $j, k$  the smoothed classifier  $g$  has class probability that satisfy*

$$q(y_A | \phi(x, z_{jk}); \epsilon) \geq p_A^{(jk)} > p_B^{(jk)} \geq \max_{y \neq y_A} q(y | \phi(x, z_{jk}); \epsilon) \quad (18)$$

*Then it is guaranteed that  $y_A = \arg \max_y q(y | \phi(x, z); \epsilon)$  if  $\forall j, k$  and  $\forall z \in S$ ,*

$$\frac{\sigma}{2} \left( \Phi^{-1}(p_A^{(jk)}) - \Phi^{-1}(p_B^{(jk)}) \right) \geq \frac{\sqrt{N(4\varphi^2 + 8\varphi + 5)}}{2M}. \quad (19)$$

We also consider the composition of three transformations: z-twist  $\circ$  z-taper  $\circ$  z-rotation.

**Theorem 4.** *We define the composite transformation z-twist  $\circ$  z-taper  $\circ$  z-rotation by  $\phi : \mathcal{X} \times \mathcal{Z} \rightarrow \mathcal{X}$ , with input space  $\mathcal{X} = \mathbb{R}^{3 \times N}$  and parameter space  $\mathcal{Z} = \mathcal{Z}_{Twist} \times \mathcal{Z}_{Taper} \times \mathcal{Z}_{Rot-z} = \mathbb{R}^3$ . Let  $g : \mathcal{X} \rightarrow \mathcal{Y}$  be a classifier smoothed by random noises  $\epsilon \sim \mathcal{N}(0, \sigma^2 \mathbb{1}_{3 \times N})$ , which predicts  $g(x; \epsilon) = \arg \max_y q(y | x; \epsilon) = \arg \max_y \mathbb{E}(p(y | x + \epsilon))$ .*

*Let  $\{z_{jkl} \in \mathcal{Z} : z = (\varphi_j, \alpha_k, \theta_l)\}$  be a set of parameters with  $\varphi_j = \frac{2j}{M} - \varphi$ ,  $\alpha_k = \frac{2k}{M} - \alpha$  and  $\theta_l = \frac{2l}{M} - \theta$ . Therefore  $(\varphi_j, \alpha_k, \theta_l)$  distribute uniformly in the subspace  $\mathcal{Z}_{robust} = [-\varphi, \varphi] \times [-\alpha, \alpha] \times [-\theta, \theta] \subseteq \mathcal{Z}$ . Suppose for any  $j, k, l$ , the smoothed classifier  $g$  has class probability that satisfy*

$$\begin{aligned} q(y_A | \phi(x, z_{jkl}); \epsilon) &\geq p_A^{(jkl)} > p_B^{(jkl)} \\ &\geq \max_{y \neq y_A} q(y | \phi(x, z_{jkl}); \epsilon) \end{aligned} \quad (20)$$

*Then it is guaranteed that for any  $z \in \mathcal{Z}_{robust} : y_A = \arg \max_y q(y | \phi(x, z); \epsilon)$ , if for any  $i, j, k$ ,*

$$\frac{\sigma}{2} \left( \Phi^{-1}(p_A^{(jkl)}) - \Phi^{-1}(p_B^{(jkl)}) \right) \geq \frac{\sqrt{N(1 + \frac{27}{4}(1 + \alpha)^2)}}{2M} \quad (21)$$

Both Theorem 3 and Theorem 4 are based on our proposed approach of sampling parameters in the parameter space and certifying the neighboring distributions of the samples separately by bounding the interpolation error Equation (29). These two theorems are rigorously proved in Appendix B.4 and Appendix B.5.

## 5. Experiments

We conduct extensive experiments on different 3D semantic transformations and models to evaluate the certified robustness derived from our TPC framework. We show that TPC significantly outperform the-state-of-the-art in terms of the certified robustness against a range of semantic transformations, and the results also lead to some interesting findings.

### 5.1. Experimental setup

**Dataset.** We perform experiments on the ModelNet40 dataset (Wu et al., 2015), which includes different 3D objects of 40 categories. We follow the standard pre-processing pipeline that places the point clouds to the center and scales them into a unit sphere.

We also conduct experiments for part segmentation task, for which the ShapeNet dataset (Chang et al., 2015) is used for evaluation. It contains 16681 meshes from 16 categories and also 50 predefined part labels. The experiment results are presented in Section 5.2.4.

**Models.** We run our experiments for point cloud classification on PointNet models (Qi et al., 2017) with different point cloud sizes. We apply data augmentation training for each transformation combined with consistency regularization to train base classifiers. We then employ our TPC framework to smooth these models and derive robustness certification bounds against various transformations.

**Evaluation Metrics.** To evaluate the robustness of point clouds classification, we pick a fixed random subset of ModelNet40 test dataset. We report the **certified accuracy** defined by the fraction of point clouds that are classified both *correctly* and *consistently* within certain transformation space. The baseline we compare with (Lorenz et al., 2021) only presents **certified ratio**, which is the fraction of test samples classified *consistently*. We believe that the *certified accuracy* is a more rigorous metric for evaluation based on existing standard certification protocols in the image domain (Cohen et al., 2019a). We thus calculate the certified accuracy for baselines based on the results reported in the paper (Lorenz et al., 2021) for comparison. Besides,

we also report the certified ratio comparison in Table 2 and Appendix D.

For part segmentation task, we evaluate our method using the a fixed random subset of ShapeNet test dataset. As the part segmentation task requires assigning a part category to each point in a point cloud, we report the **point-wise certified accuracy** defined as the fraction of points that are classified *correctly* and *consistently*. Note that other common metrics such as IoU can be easily derived based on our bound as well, which we will focus on the point-wise certified accuracy for the convenience of comparison with baseline (Lorenz et al., 2021).

## 5.2. Main Results

In this section, we present our main experimental results. Concretely, we show that: (1) the certified accuracy of TPC under a range of semantic transformations is significantly higher than the baseline, and TPC is able to certify under some transformation space where the baseline cannot be applied; (2) the certified accuracy of TPC always outperforms the baseline for different point cloud sizes, and more interestingly, the certified accuracy of TPC increases with the increasing of point cloud size while that of the baseline decreases due to relaxation; (3) TPC is also capable of certifying against  $\ell_2$  or  $\ell_\infty$  norm bounded 3D perturbations for different point clouds sizes; (4) on the part segmentation task, TPC still outperforms the baseline against different semantic transformations and is able to certify some transformation parameter space that the baseline is not applicable.

### 5.2.1. COMPARISON OF CERTIFIED ACCURACY

Table 1 shows the certified accuracy we achieved for different transformations compared with prior works. We train a PointNet model with 64 points, which is consistent with the baseline. For transformations characterized by one parameter, such as z-rotation, z-twist and z-taper, we report the certified accuracy against attacks in  $\pm\theta$ . For z-shear with a parameter space of  $\mathbb{R}^2$ , we report the certified accuracy against attacks in certain  $\ell_2$  parameter radius.

The highlighted results in Table 1 demonstrates that our framework TPC significantly outperforms the state of the art in every known semantic transformations. For example, we improve the certified accuracy from 59.8% to 83.4% for z-shear in  $\pm 0.03$  and from 20.3% to 83.8% for z-twist in  $\pm 20^\circ$ .

Besides, we also report the certified accuracy for larger attack radius for which the baseline cannot certify (cells with “-”). For instance, we achieve 81.3% certified accuracy on z-rotation within  $\pm 180^\circ$ , which is essentially every possible z-rotation transformation.

The general rotation transformations we define in Sec-

Table 1. Comparison of certified accuracy achieved by our transformation specific smoothing framework TPC and the baseline, DeepG3D (Lorenz et al., 2021). “-” denotes the settings where the baselines cannot scale up to.

Transformation	Attack radius	Certified Accuracy (%)	
		TPC	DeepG3D
ZYX-rotation	$2^\circ$	<b>81.4</b>	61.6
	$5^\circ$	<b>69.2</b>	49.6
General rotation	$5^\circ$	<b>78.5</b>	-
	$10^\circ$	<b>69.2</b>	-
	$15^\circ$	<b>55.5</b>	-
Z-rotation	$20^\circ$	<b>84.2</b>	81.8
	$60^\circ$	<b>83.8</b>	81.0
	$180^\circ$	<b>81.3</b>	-
Z-shear	0.03	<b>83.4</b>	59.8
	0.1	<b>82.2</b>	-
	0.2	<b>77.7</b>	-
Z-twist	$20^\circ$	<b>83.8</b>	20.3
	$60^\circ$	<b>80.1</b>	-
	$180^\circ$	<b>64.3</b>	-
Z-taper	0.1	<b>78.1</b>	69.0
	0.2	<b>76.5</b>	23.9
	0.5	<b>66.0</b>	-
Z-twist $\circ$ Z-rotation	$20^\circ, 1^\circ$	<b>78.9</b>	13.8
	$20^\circ, 5^\circ$	<b>78.5</b>	-
	$50^\circ, 5^\circ$	<b>76.9</b>	-
Z-taper $\circ$ Z-rotation	$0.1, 1^\circ$	<b>76.1</b>	58.2
	$0.2, 1^\circ$	<b>72.9</b>	17.5
Z-twist $\circ$ Z-taper $\circ$ Z-rotation	$10^\circ, 0.1, 1^\circ$	<b>68.8</b>	17.5
	$20^\circ, 0.2, 1^\circ$	<b>63.1</b>	4.6

Table 2. Comparison of certified ratio as well as certified accuracy for z-rotation transformations. “-” denotes the settings where the baselines cannot scale up to.

Radius	Certified Ratio (%)		Certified Accuracy (%)	
	TPC	DeepG3D	TPC	DeepG3D
$20^\circ$	<b>99.0</b>	96.7	<b>84.2</b>	81.8
$60^\circ$	<b>98.1</b>	95.7	<b>83.8</b>	81.0
$180^\circ$	<b>95.2</b>	-	<b>81.3</b>	-

tion 4.3 includes rotations along any axis with bounded angles. Lorenz et al. consider *ZYX-rotation*, the composition of three rotations within  $\pm\theta$  (Euler angles) along  $x, y, z$  axes instead (2021), which results in a different geometric shape for the certified parameter space. However, the parameter space restricted by  $S^2 \times [0, 2\theta]$  of general rotation strictly contains the space defined by  $\pm\theta$  for three Euler angles. (See Appendix B.3 for proof.) The derived results for ZYX-rotation are also shown in Table 1 for comparison.

**Comparison of Certified Ratio.** Aside from the certified accuracy, we also consider certified ratio as another metric according to the baseline. This metric measures the tightness of certification bounds, but fails to take the classification accuracy into account which is important. Therefore, we mainly present the comparison based on certified ratio for z-rotations in Table 2 only for comparison, and leave the full comparison in Appendix D.

Table 3. Certification of z-rotation for different point cloud sizes. The certified accuracy achieved by our TPC increases as the size of point cloud model increases.

(a)  $\theta = \pm 3^\circ$  compared with DeepG3D (Lorenz et al., 2021)

Points	16	32	64	128	256	512	1024
TPC	<b>83.2</b>	<b>83.8</b>	<b>86.6</b>	<b>87.4</b>	<b>89.4</b>	<b>89.8</b>	<b>90.5</b>
DeepG3D	75.4	78.4	79.1	69.4	57.5	42.8	32.3

(b) Certified accuracy of TPC under  $\theta = \pm 180^\circ$

Points	16	32	64	128	256	512	1024
TPC	73.6	79.3	81.3	81.8	83.0	84.6	83.8

### 5.2.2. CERTIFICATION ON POINT CLOUDS WITH DIFFERENT SIZES

Here we show that our certification framework naturally scales up to larger point cloud models. A basic principle of our TPC framework is that deriving the certification bound for a smoothed classifier only depends on the predicted class probability. In other words, it does not rely on specific model architectures.

The relaxation based verifiers (Lorenz et al., 2021; Singh et al., 2019) have worse certification guarantees for larger point clouds due to the precision loss during relaxation, especially for pooling layers that are heavily used in point cloud model architectures. For example, the DeepG3D verifier guarantees 79.1% certified accuracy for a 64-point model on z-rotation with  $\pm 3^\circ$  (without splitting); but the certification drops to 32.3% for an 1024-point model (Lorenz et al., 2021). In contrast, using our TPC framework, the certified accuracy tends to **increase** with larger number of points in point clouds. This is because larger PointNet models predict more accurately and yield higher class probability after smoothing. We compare our TPC framework with the baseline in terms of certified accuracy for different point cloud sizes in Table 3a. The baseline DeepG3D only presents results for z-rotations in  $\theta = \pm 3^\circ$ , which cannot fully illustrate the capability of our method. Therefore, we also report our experimental results for z-rotations in  $\theta = \pm 180^\circ$  in Table 3b. It shows that our method can scale up to larger point cloud models to accommodate real-world scenarios.

### 5.2.3. CERTIFICATION AGAINST $\ell_p$ NORM BOUNDED 3D-PERTURBATIONS

In addition to semantic transformations, we also provide robustness certification for point cloud models against  $\ell_2$  perturbations. For a point cloud with  $N$  points,  $x \in \mathbb{R}^{3 \times N}$ , we smooth the model based on TPC and certify its robustness against  $\ell_2$  perturbations.

We cannot directly certify against perturbations with bounded  $\ell_\infty$  norm. However, a certification bound similar to the baseline (Lorenz et al., 2021) can still be derived, using the loose inequality  $\|\theta\|_\infty \leq \sqrt{3N}\|\theta\|_2$ . Here, we exhibit

Table 4. Certified accuracy of TPC for point cloud models under  $\ell_2$  attacks. The certified accuracy increases as the size of point cloud models increases.

Attack	Radius	Certified Accuracy (%)		
		16	64	256
$\ell_2$	0.05	74.1	82.2	84.2
$\ell_2$	0.1	61.9	70.8	77.3

Table 5. Comparison of point-wise certified accuracy for the *part segmentation* task. “-” denotes the settings that the baseline does not consider or cannot scale up to.

Transformation	Radius	Certified Accuracy (%)	
		TPC	DeepG3D
Z-rotation	$5^\circ$	<b>87.8</b>	85.7
Z-rotation	$10^\circ$	<b>86.1</b>	84.8
Z-rotation	$180^\circ$	<b>70.8</b>	-
Z-shear	0.2	<b>86.1</b>	-
Z-twist	$180^\circ$	<b>74.5</b>	-

the certified accuracy for bounded  $\ell_2$  norm in Table 4; and omit more details for  $\ell_\infty$  norm to Appendix C. We show that under the  $\ell_2$  norm bounded 3D-perturbations, TPC certifies even better as the point clouds sizes increase and achieve a high certified accuracy of 77.3% for perturbations with  $\ell_2$  norm bounded by 0.1.

### 5.2.4. CERTIFICATION FOR PART SEGMENTATION

Part segmentation is a common 3D recognition task in which a model is in charge of assigning each point or face of a 3D mesh to one of the predefined categories. As our TPC framework is independent from concrete model architectures, it can be naturally extended to handle the part segmentation task.

We evaluate our method using the ShapeNet part dataset from (Chang et al., 2015). We train a segmentation version PointNet (Qi et al., 2017) with 64 points, which predicts a part category for each point in the point cloud. The certified accuracy reported in Table 5 denotes the percentage of points guaranteed to be labeled correctly. We can see that for the part segmentation task, TPC consistently outperforms the baseline against different semantic transformations. The baseline only reports the result for z-rotations in  $\pm 5^\circ$  and  $\pm 10^\circ$ , while we present robustness guarantees for any z-rotation ( $\pm 180^\circ$ ) as well as other transformations including shearing and twisting.

## 6. Conclusions

In this work we propose a unified certification framework TPC for point cloud models against a diverse range of semantic transformations. Our theoretical and empirical analysis show that TPC is more scalable and able to provide much tighter certification under different settings and tasks.

## References

- Aoki, Y., Goforth, H., Srivatsan, R. A., and Lucey, S. Pointnetk: Robust & efficient point cloud registration using pointnet. In *Proceedings of the IEEE/CVF Conference on Computer Vision and Pattern Recognition*, pp. 7163–7172, 2019.
- Balunović, M., Baader, M., Singh, G., Gehr, T., and Vechev, M. Certifying geometric robustness of neural networks. *Advances in Neural Information Processing Systems 32*, 2019.
- Cao, Y., Xiao, C., Cyr, B., Zhou, Y., Park, W., Rampazzi, S., Chen, Q. A., Fu, K., and Mao, Z. M. Adversarial sensor attack on lidar-based perception in autonomous driving. In *Proceedings of the 2019 ACM SIGSAC conference on computer and communications security*, pp. 2267–2281, 2019.
- Cao, Y., Wang, N., Xiao, C., Yang, D., Fang, J., Yang, R., Chen, Q. A., Liu, M., and Li, B. Invisible for both camera and lidar: Security of multi-sensor fusion based perception in autonomous driving under physical-world attacks. In *2021 IEEE Symposium on Security and Privacy (SP)*, pp. 176–194. IEEE, 2021.
- Chang, A. X., Funkhouser, T. A., Guibas, L. J., Hanrahan, P., Huang, Q., Li, Z., Savarese, S., Savva, M., Song, S., Su, H., Xiao, J., Yi, L., and Yu, F. Shapenet: An information-rich 3d model repository. *CoRR*, abs/1512.03012, 2015. URL <http://arxiv.org/abs/1512.03012>.
- Chen, S., Liu, B., Feng, C., Vallespi-Gonzalez, C., and Wellington, C. 3d point cloud processing and learning for autonomous driving: Impacting map creation, localization, and perception. *IEEE Signal Processing Magazine*, 38(1):68–86, 2020.
- Chen, X., Ma, H., Wan, J., Li, B., and Xia, T. Multi-view 3d object detection network for autonomous driving. In *Proceedings of the IEEE conference on Computer Vision and Pattern Recognition*, pp. 1907–1915, 2017.
- Cohen, J., Rosenfeld, E., and Kolter, Z. Certified adversarial robustness via randomized smoothing. In Chaudhuri, K. and Salakhutdinov, R. (eds.), *Proceedings of the 36th International Conference on Machine Learning*, volume 97 of *Proceedings of Machine Learning Research*, pp. 1310–1320. PMLR, 09–15 Jun 2019a. URL <https://proceedings.mlr.press/v97/cohen19c.html>.
- Cohen, J., Rosenfeld, E., and Kolter, Z. Certified adversarial robustness via randomized smoothing. In *International Conference on Machine Learning*, pp. 1310–1320. PMLR, 2019b.
- Eykholt, K., Evtimov, I., Fernandes, E., Li, B., Rahmati, A., Xiao, C., Prakash, A., Kohno, T., and Song, D. Robust physical-world attacks on deep learning visual classification. In *Proceedings of the IEEE Conference on Computer Vision and Pattern Recognition*, pp. 1625–1634, 2018.
- Fang, J., Yang, R., Chen, Q. A., Liu, M., Li, B., et al. Invisible for both camera and lidar: Security of multi-sensor fusion based perception in autonomous driving under physical-world attacks. *arXiv preprint arXiv:2106.09249*, 2021.
- Fischer, M., Baader, M., and Vechev, M. Certified defense to image transformations via randomized smoothing. *Advances in Neural Information Processing Systems 33 proceedings (NeurIPS 2020)*, 2020.
- Hendrycks, D. and Dietterich, T. Benchmarking neural network robustness to common corruptions and perturbations. In *International Conference on Learning Representations*, 2018.
- Li, B. 3d fully convolutional network for vehicle detection in point cloud. In *2017 IEEE/RSJ International Conference on Intelligent Robots and Systems (IROS)*, pp. 1513–1518. IEEE, 2017.
- Li, H., Xu, X., Zhang, X., Yang, S., and Li, B. Qeba: Query-efficient boundary-based blackbox attack. In *Proceedings of the IEEE/CVF Conference on Computer Vision and Pattern Recognition*, pp. 1221–1230, 2020a.
- Li, H., Li, L., Xu, X., Zhang, X., Yang, S., and Li, B. Non-linear gradient estimation for query efficient blackbox attack. In *International Conference on Artificial Intelligence and Statistics (AISTATS 2021)*, Proceedings of Machine Learning Research. PMLR, 13–15 Apr 2021a.
- Li, L., Zhong, Z., Li, B., and Xie, T. Robustra: Training provable robust neural networks over reference adversarial space. In *Proceedings of the Twenty-Eighth International Joint Conference on Artificial Intelligence (IJCAI 2019)*, pp. 4711–4717. International Joint Conferences on Artificial Intelligence Organization, 7 2019. doi: 10.24963/ijcai.2019/654. URL <https://doi.org/10.24963/ijcai.2019/654>.
- Li, L., Xie, T., and Li, B. Sok: Certified robustness for deep neural networks. *arXiv preprint arXiv:2009.04131*, 2020b.
- Li, L., Weber, M., Xu, X., Rimanic, L., Kailkhura, B., Xie, T., Zhang, C., and Li, B. TSS: transformation-specific smoothing for robustness certification. In Kim, Y., Kim, J., Vigna, G., and Shi, E. (eds.), *CCS '21: 2021 ACM SIGSAC Conference on Computer and Communications Security, Virtual Event, Republic of Korea*,

- November 15 - 19, 2021, pp. 535–557. ACM, 2021b. doi: 10.1145/3460120.3485258. URL <https://doi.org/10.1145/3460120.3485258>.
- Liu, H., Jia, J., and Gong, N. Z. Pointguard: Provably robust 3d point cloud classification. In *Proceedings of the IEEE/CVF Conference on Computer Vision and Pattern Recognition*, pp. 6186–6195, 2021.
- Lorenz, T., Ruoss, A., Balunovic, M., Singh, G., and Vechev, M. T. Robustness certification for point cloud models. *CoRR*, abs/2103.16652, 2021. URL <https://arxiv.org/abs/2103.16652>.
- Mirman, M., Gehr, T., and Vechev, M. Differentiable abstract interpretation for provably robust neural networks. In *International Conference on Machine Learning*, pp. 3578–3586. PMLR, 2018.
- Pei, K., Cao, Y., Yang, J., and Jana, S. Deepxplore: Automated whitebox testing of deep learning systems. In *proceedings of the 26th Symposium on Operating Systems Principles*, pp. 1–18, 2017.
- Qi, C. R., Su, H., Mo, K., and Guibas, L. J. Pointnet: Deep learning on point sets for 3d classification and segmentation. In *Proceedings of the IEEE conference on computer vision and pattern recognition*, pp. 652–660, 2017.
- Qiu, H., Xiao, C., Yang, L., Yan, X., Lee, H., and Li, B. Semanticadv: Generating adversarial examples via attribute-conditioned image editing. In *European Conference on Computer Vision*, pp. 19–37. Springer, 2020.
- Salman, H., Yang, G., Li, J., Zhang, P., Zhang, H., Razenshteyn, I., and Bubeck, S. Provably robust deep learning via adversarially trained smoothed classifiers. In *Proceedings of the 33rd International Conference on Neural Information Processing Systems*, pp. 11292–11303, 2019.
- Singh, G., Gehr, T., Püschel, M., and Vechev, M. An abstract domain for certifying neural networks. *Proc. ACM Program. Lang.*, 3(POPL), jan 2019. doi: 10.1145/3290354. URL <https://doi.org/10.1145/3290354>.
- Sun, J., Cao, Y., Chen, Q. A., and Mao, Z. M. Towards robust lidar-based perception in autonomous driving: General black-box adversarial sensor attack and countermeasures. In *29th {USENIX} Security Symposium ({USENIX} Security 20)*, pp. 877–894, 2020.
- Szegedy, C., Zaremba, W., Sutskever, I., Bruna, J., Erhan, D., Goodfellow, I., and Fergus, R. Intriguing properties of neural networks. *arXiv preprint arXiv:1312.6199*, 2013.
- Tramer, F., Carlini, N., Brendel, W., and Madry, A. On adaptive attacks to adversarial example defenses. *Advances in Neural Information Processing Systems*, 33, 2020.
- Tsuzuku, Y., Sato, I., and Sugiyama, M. Lipschitz-margin training: scalable certification of perturbation invariance for deep neural networks. In *Proceedings of the 32nd International Conference on Neural Information Processing Systems*, pp. 6542–6551, 2018.
- Wang, Y., Sun, Y., Liu, Z., Sarma, S. E., Bronstein, M. M., and Solomon, J. M. Dynamic graph cnn for learning on point clouds. *Acm Transactions On Graphics (tog)*, 38(5):1–12, 2019.
- Weng, L., Zhang, H., Chen, H., Song, Z., Hsieh, C.-J., Daniel, L., Boning, D., and Dhillon, I. Towards fast computation of certified robustness for relu networks. In *International Conference on Machine Learning*, pp. 5276–5285. PMLR, 2018.
- Wong, E. and Kolter, Z. Provable defenses against adversarial examples via the convex outer adversarial polytope. In *International Conference on Machine Learning*, pp. 5286–5295. PMLR, 2018.
- Wong, E., Schmidt, F. R., Metzen, J. H., and Kolter, J. Z. Scaling provable adversarial defenses. In *NeurIPS*, 2018.
- Wu, Z., Song, S., Khosla, A., Yu, F., Zhang, L., Tang, X., and Xiao, J. 3d shapenets: A deep representation for volumetric shapes. In *Proceedings of the IEEE conference on computer vision and pattern recognition*, pp. 1912–1920, 2015.
- Xiang, C., Qi, C. R., and Li, B. Generating 3d adversarial point clouds. In *Proceedings of the IEEE/CVF Conference on Computer Vision and Pattern Recognition*, pp. 9136–9144, 2019.
- Xiao, C., Deng, R., Li, B., Yu, F., Liu, M., and Song, D. Characterizing adversarial examples based on spatial consistency information for semantic segmentation. In *Proceedings of the European Conference on Computer Vision (ECCV)*, pp. 217–234, 2018.
- Xiao, C., Yang, D., Li, B., Deng, J., and Liu, M. Meshadv: Adversarial meshes for visual recognition. In *Proceedings of the IEEE/CVF Conference on Computer Vision and Pattern Recognition*, pp. 6898–6907, 2019.
- Yang, G., Duan, T., Hu, J. E., Salman, H., Razenshteyn, I., and Li, J. Randomized smoothing of all shapes and sizes. In *International Conference on Machine Learning*, pp. 10693–10705. PMLR, 2020.
- Zhang, B., Cai, T., Lu, Z., He, D., and Wang, L. Towards certifying l-infinity robustness using neural networks with l-inf-dist neurons. In *International Conference on Machine Learning*, pp. 12368–12379. PMLR, 2021.

Zhang, H., Weng, T.-W., Chen, P.-Y., Hsieh, C.-J., and Daniel, L. Efficient neural network robustness certification with general activation functions. *Advances in Neural Information Processing Systems*, 31:4939–4948, 2018.

Zhang, J., Li, L., Li, H., Zhang, X., Yang, S., and Li, B. Progressive-scale boundary blackbox attack via projective gradient estimation. *ICML*, 2022.

Zhou, Y. and Tuzel, O. Voxelnet: End-to-end learning for point cloud based 3d object detection. In *Proceedings of the IEEE conference on computer vision and pattern recognition*, pp. 4490–4499, 2018.

Zhu, Q., Li, Y., Hu, H., and Wu, B. Robust point cloud classification based on multi-level semantic relationships for urban scenes. *ISPRS journal of photogrammetry and remote sensing*, 129:86–102, 2017.

## A. Generic Theorems for Composable and Indirectly Composable Transformations

### A.1. Main Theorem for Transformation Specific Smoothing

**Theorem 5** (Theorem 1 (Li et al., 2021b)). *Let  $\epsilon_0 \sim \mathbb{P}_0$  and  $\epsilon_1 \sim \mathbb{P}_1$  be  $\mathcal{Z}$ -valued random variables with probability density function  $f_0$  and  $f_1$ . Let  $\phi : \mathcal{X} \times \mathcal{Z} \rightarrow \mathcal{X}$  be a semantic transformation. Suppose a classifier smoothed by the transformation  $\phi$  predicts  $y_A = g(x; \epsilon)$ , and that*

$$q(y_A|x, \epsilon) \geq p_A > p_B \geq \max_{y \neq y_A} q(y|x, \epsilon). \quad (22)$$

For  $t \geq 0$ , we define sets  $\underline{S}_t, \bar{S}_t \subseteq \mathcal{Z}$  by  $\underline{S}_t := \{f_1/f_0 < t\}$  and  $\bar{S}_t := \{f_1/f_0 \leq t\}$ . Also define a function  $\xi : [0, 1] \rightarrow [0, 1]$  by

$$\xi(p) := \sup\{\mathbb{P}_1(S) : \underline{S}_{\tau_p} \subseteq S \subseteq \bar{S}_{\tau_p}\} \quad (23)$$

$$\text{where } \tau_p := \inf\{t \geq 0 : \mathbb{P}_0(\bar{S}_t) \geq p\}. \quad (24)$$

Then it is guaranteed that  $g(x; \epsilon_1) = g(x; \epsilon_0)$  if the following condition holds:

$$\xi(p_A) + \xi(1 - p_B) > 1. \quad (25)$$

Intuitively,  $\xi(p_A)$  computes a lower bound for the class probability of  $y_A$  when the smoothing distribution changes from  $\epsilon_0$  to  $\epsilon_1$ . Suppose we want to certify an  $\epsilon_0$ -smoothed classifier against an composable transformation  $\phi$  and  $\phi(\phi(x, \alpha), \beta) = \phi(x, \gamma_\alpha(\beta))$ . For any attack  $\alpha \in \mathcal{Z}$ , we assign  $\epsilon_1 = \gamma_\alpha(\epsilon_0)$  and check for the condition of Equation (25). Moreover, if  $\phi$  is additive and  $\epsilon_0$  is a Gaussian random variable, we have the following corollary:

**Corollary 3** (Corollary 7 (Li et al., 2021b)). *Let  $\phi : \mathcal{X} \times \mathcal{Z} \rightarrow \mathcal{X}$  be an additive transformation and  $\mathcal{Z} = \mathbb{R}^m$ . Suppose classifier  $g$  is smoothed by a random variable  $\epsilon_0 \sim \mathcal{N}(0, \text{diag}(\sigma_1^2, \dots, \sigma_m^2))$ . Assume that the class probability satisfies:*

$$q(y_A|x, \epsilon_0) \geq p_A > p_B \geq \max_{y \neq y_A} q(y|x, \epsilon_0). \quad (26)$$

Then it holds that  $g(x; \epsilon_0) = g(\phi(x, \alpha); \epsilon)$  if the attack parameter  $\alpha$  satisfies:

$$\sqrt{\sum_{i=1}^m \left(\frac{\alpha_i}{\sigma_i}\right)^2} < \frac{1}{2} \left( \Phi^{-1}(p_A) - \Phi^{-1}(p_B) \right). \quad (27)$$

We direct readers to (Li et al., 2021b) for the rigorous proof on Theorem 5 and Corollary 3 .

### A.2. Theorem for Certifying Indirectly Composable Transformations

**Theorem 6** (Corollary 2 (Li et al., 2021b)). *Let  $\psi(x, \delta) = x + \delta$  and  $\epsilon \sim \mathcal{N}(0, \sigma^2 \mathbf{1}_d)$ .  $\phi : \mathbb{X} \times \mathcal{Z}_\phi \rightarrow \mathcal{X}$  is a indirectly composable transformation. Construct a smoothed classifier with additive noise  $\psi(x, \delta)$  and suppose it predicts  $y = \arg \max_{y \in \mathcal{Y}} q(y|x; \epsilon)$ . Draw  $N$  samples  $\{\alpha_i\}_i^N$  from a set  $\mathcal{S} \subseteq \mathcal{Z}_\phi$ . Assume*

$$q(y_A|\phi(x, \alpha_i), \epsilon) \geq p_A^{(i)} \geq p_B^{(i)} \geq \max_{y \neq y_A} q(y|\phi(x, \alpha_i), \epsilon). \quad (28)$$

Then it is guaranteed that  $\forall \alpha \in \mathcal{S} : y_A = \arg \max_{y \in \mathcal{Y}} q(y|\phi(x, \alpha); \epsilon)$  if the maximum interpolation error

$$\mathcal{M}_\mathcal{S} := \max_{\alpha \in \mathcal{S}} \min_{1 \leq i \leq N} \mathcal{M}(\alpha, \alpha_i) \quad (29)$$

$$= \max_{\alpha \in \mathcal{S}} \min_{1 \leq i \leq N} \|\phi(x, \alpha) - \phi(x, \alpha_i)\|_2 \quad (30)$$

$$\text{satisfies } \mathcal{M}_\mathcal{S} < R := \frac{\sigma}{2} \min_{1 \leq i \leq N} \left( \Phi^{-1}(p_A^{(i)}) - \Phi^{-1}(p_B^{(i)}) \right) \quad (31)$$

## B. Proofs for Certifying Specific Transformations

Here, we present proofs for the theorems and corollaries proposed in Section 4, including concrete protocols for common 3D transformations, such as z-rotation, z-twist, z-taper, etc.

### B.1. Proof of Theorem 1: Certifying Z-taper

*Proof.* The z-taper transformation is defined as  $\phi_{TP} : \mathcal{X} \times \mathbb{R} \rightarrow \mathcal{X}$  where  $\mathcal{X} = \mathbb{R}^{3 \times N}$  is the space for input point clouds. A z-taper transformation acting on a point cloud  $x = \{p_i\}_{i=1}^N \in \mathcal{X}$  in fact performs point-wise transformation to each  $p_i$ , where

$$\phi_{TP}(p_i, \theta) = \begin{pmatrix} x_i(1 + \theta z_i) \\ y_i(1 + \theta z_i) \\ z_i \end{pmatrix}, \text{ if } p_i = (x_i, y_i, z_i)^T. \quad (32)$$

We calculate the interpolation error between two parameters  $\theta$  and  $\theta_j$  by

$$\mathcal{M}(\theta, \theta_j) = \|\phi_{TP}(x, \theta) - \phi_{TP}(x, \theta_j)\|_2 \quad (33)$$

$$= \left( \sum_{i=1}^N \|\phi_{TP}(p_i, \theta) - \phi_{TP}(p_i, \theta_j)\|_2^2 \right)^{1/2} \quad (34)$$

$$= \left( \sum_{i=1}^N (x_i^2 + y_i^2) z_i^2 (\theta - \theta_j)^2 \right)^{1/2} \quad (35)$$

$$\leq \frac{\sqrt{N} |\theta - \theta_j|}{2}. \quad (36)$$

The last inequality holds because we assume point clouds are normalized into a unit ball, so  $(x_i^2 + y_i^2) z_i^2 \leq \frac{1}{4}$ . Recall that we choose  $\theta_j = (\frac{2j}{M} - 1)R$  and  $j = 0, 1, \dots, M$ . Hence,  $\max_{\theta \in [-R, R]} \min_j |\theta - \theta_j| < \frac{R}{M}$ . The maximal interpolation error is thus bounded by

$$\mathcal{M}_S = \max_{\theta \in [-R, R]} \min_j \mathcal{M}(\theta, \theta_j) \quad (37)$$

$$\leq \frac{R\sqrt{N}}{2M}. \quad (38)$$

According to Theorem 6, it is guaranteed for all  $\theta \in [-R, R]$  that  $y_A = \arg \max_y q(y | \phi_{TP}(x, \theta); \epsilon)$ , if  $\forall j$ ,

$$\frac{\sigma}{2} \left( \Phi^{-1}(p_A^{(j)}) - \Phi^{-1}(p_B^{(j)}) \right) \geq \frac{R\sqrt{N}}{2M}. \quad (39)$$

### B.2. Proof of Theorem 2: Certifying General Rotation

*Proof.* We first recall the definition of general rotation:  $\phi_R : \mathcal{X} \times \mathcal{Z} \rightarrow \mathcal{X}$ . The parameter space  $\mathcal{Z} = S^2 \times \mathbb{R}^+$  where  $S^2$  characterizes the rotation axis and  $\mathbb{R}^+$  stands for the rotation angle. By Euler's theorem, general rotations are composable transformations; and the composition of two rotations can be expressed by:

$$\phi_R(\phi_R(x, z_1), z_2) = \phi_R(x, z_3) \quad (40)$$

$$\text{where } \begin{cases} k_3 = \text{normalize}(\sin \frac{\theta_1}{2} \cos \frac{\theta_2}{2} k_1 + \cos \frac{\theta_1}{2} \sin \frac{\theta_2}{2} k_2 + \sin \frac{\theta_1}{2} \sin \frac{\theta_2}{2} k_2 \times k_1) \\ \theta_3 = 2 \arccos(\cos \frac{\theta_1}{2} \cos \frac{\theta_2}{2} - \sin \frac{\theta_1}{2} \sin \frac{\theta_2}{2} k_1 \cdot k_2) \end{cases} \quad (41)$$

The interpolation error of a point cloud  $x = \{p_i\}_{i=1}^N$  between two transformations with parameters  $z = (k, \theta)$  and  $z_j = (k_j, \theta_j)$  is bounded by:

$$\mathcal{M}(z, z_j) = \|\phi_R(x, z) - \phi_R(x, z_j)\|_2 \quad (42)$$

$$= \|\phi_R(\phi_R(x, z), z_j^{-1}) - x\|_2, \quad (\text{where } z_j^{-1} = (-k_j, \theta_j)) \quad (43)$$

$$= \left( \sum_{i=1}^N \|\phi_R(\phi_R(p_i, z), z_j^{-1}) - p_i\|_2^2 \right)^{1/2} \quad (44)$$

$$= \left( \sum_{i=1}^N \|\phi_R(p_i, z') - p_i\|_2^2 \right)^{1/2} \quad (\text{Let } z' = (k', \theta') \text{ be the composition of } z, z_j^{-1}) \quad (45)$$

$$\leq \left( \sum_{i=1}^N (\theta' \|p_i\|_2)^2 \right)^{1/2} = \theta' \|x\|_2. \quad (46)$$

Assuming  $\langle k, k_i \rangle \leq \epsilon$ ,  $|\theta - \theta_i| \leq \delta$ , we derive that for  $\theta, \theta_i \in [0, R]$ ,

$$\cos \frac{\theta'}{2} = \cos \frac{\theta_j}{2} \cos \frac{\theta}{2} + \cos \langle k, k_i \rangle \sin \frac{\theta_j}{2} \sin \frac{\theta}{2}, \quad (\langle k, k_i \rangle \leq \epsilon) \quad (47)$$

$$\geq \cos \frac{\theta_j - \theta}{2} - \frac{\epsilon^2}{2} \sin \frac{\theta_j}{2} \sin \frac{\theta}{2} \quad (\text{since } \cos \epsilon \geq 1 - \frac{\epsilon^2}{2}) \quad (48)$$

$$\geq 1 - \left( \frac{\theta_j - \theta}{2} \right)^2 - \frac{\epsilon^2 \theta \theta_j}{8}. \quad (\text{since } \sin x \leq x) \quad (49)$$

$$\geq 1 - \frac{\delta^2}{4} - \frac{\epsilon^2 R^2}{8}. \quad (50)$$

Note that  $\arccos(1 - x) \leq \frac{\pi}{2} \sqrt{x}$  when  $x \in [0, 1]$ , we have

$$\theta' \leq 2 \arccos \left( 1 - \frac{\delta^2}{4} - \frac{\epsilon^2 R^2}{8} \right) \quad (51)$$

$$\leq \pi \sqrt{\frac{\delta^2}{4} + \frac{\epsilon^2 R^2}{8}}. \quad (52)$$

Combining Equation (46) and Equation (52), the maximal interpolation error for  $z \in S^2 \times [0, R]$  satisfies

$$\mathcal{M}_S = \max_z \min_j \mathcal{M}(z, z_j) \quad (53)$$

$$\leq \pi \sqrt{\frac{\delta^2}{4} + \frac{\epsilon^2 R^2}{8}} \|x\|_2. \quad (54)$$

Theorem 2 thus holds combining Equation (53) with Theorem 5.

Moreover, we specify a sampling strategy to satisfy the condition of Equation (13).

- Uniformly sample  $\pi M$  number of  $a_r \in [0, \pi]$ .
- For each  $a_r$ , uniformly sample  $2\pi M \sin \theta_s$  points  $b_{rs} \in [0, 2\pi]$ .
- Uniformly sample  $M$  number of  $\theta_t \in [0, R]$ .
- Draw  $O(M^3)$  samples in total:  $z_j = (k_j, \theta_t)$  with  $k_j = (\cos b_{rs} \sin a_r, \sin b_{rs} \sin a_r, \cos a_r)$ .

Following this strategy, the sampled parameters distribute evenly in the subspace of  $S^2 \times [0, R]$ , which guarantees  $\epsilon = \frac{\sqrt{2}}{2M}$  and  $\delta = \frac{R}{2M}$  for the conditions in Equation (13).

To sum up, it is guaranteed that for all  $z \in S^2 \times [0, R]$ ,  $x \in \mathcal{X} : y_A = \arg \max_y q(y | \phi_R(x, z); \epsilon)$ , if  $\forall j$ ,

$$\frac{\sigma}{2} \left( \Phi^{-1} \left( p_A^{(j)} \right) - \Phi^{-1} \left( p_B^{(j)} \right) \right) \geq \frac{\sqrt{2\pi R} \|x\|_2}{4M}. \quad (55)$$

*Remark.* In practise, we implement a tighter bound that  $\arccos(1 - x) \leq \sqrt{2x} + (\frac{\pi}{2} - \sqrt{2})x^{\frac{3}{2}}$  for  $x \in [0, 1]$ .

### B.3. From General Rotation to ZYX-rotation

ZYX-rotation, the composition of three rotations along  $x, y$  and  $z$  axes, is defined by:  $\phi_{ZYX-rot} : \mathcal{X} \times \mathcal{Z} \rightarrow \mathcal{X}$  with parameter space  $\mathcal{Z} = \mathbb{R}^3$ . Specifically, for  $z = (\alpha, \beta, \gamma) \in \mathcal{Z}$  and  $x = \{p_i\}_{i=1}^N \in \mathcal{X}$ ,

$$\phi_{ZYX-rot}(p_i, z) = R_z(\gamma)R_y(\beta)R_x(\alpha)p_i, \text{ where } R_z, R_y, R_x \text{ are the rotation matrix along } x, y, z \text{ axes.} \quad (56)$$

Note that the rotation angle for any rotation matrix  $R$  can be calculated by:

$$|\theta| = \arccos\left(\frac{\text{tr}(R) - 1}{2}\right) \quad (57)$$

The trace of the rotation matrix for ZYX-rotation is

$$f(\alpha, \beta, \gamma) = \text{tr}(R_z(\gamma)R_y(\beta)R_x(\alpha)) = \cos \alpha \cos \beta + \cos \alpha \cos \gamma + \cos \beta \cos \gamma - \sin \alpha \sin \beta \sin \gamma. \quad (58)$$

We assume  $\alpha, \beta, \gamma \in [-\frac{\pi}{2}, \frac{\pi}{2}]$ .  $\frac{\partial f}{\partial \alpha} = \frac{\partial f}{\partial \beta} = \frac{\partial f}{\partial \gamma} = 0$  yields  $\alpha = \beta = \gamma = 0, \pm \frac{\pi}{2}$ . Therefore, for  $\alpha, \beta, \gamma \in [-\varphi, \varphi]$  with  $\varphi \in [0, \frac{\pi}{2}]$ , the minimum of  $f(\alpha, \beta, \gamma)$  can only be on  $\alpha, \beta, \gamma = \pm \varphi$  or  $\alpha = \beta = \gamma = 0$ . Since  $\alpha = \beta = \gamma = 0$  yields the maximum  $f(\alpha, \beta, \gamma)$ , we have

$$\min_{\alpha, \beta, \gamma \in [-\varphi, \varphi]} f(\alpha, \beta, \gamma) = 3 \cos^2 \varphi - \sin^3 \varphi \quad (59)$$

Thus,

$$\cos \theta = \frac{\text{tr}(R) - 1}{2} \quad (60)$$

$$\geq \frac{3 \cos^2 \varphi - \sin^3 \varphi - 1}{2} \quad (61)$$

$$= \frac{(2 \cos^2 \varphi - 2 \sin^2 \varphi) + (\sin^2 \varphi - \sin^3 \varphi)}{2} \quad (62)$$

$$\geq \cos 2\varphi. \quad (63)$$

The rotation angle  $\theta$  is thus bounded by  $\theta \leq 2\varphi$ . Hence, any transformation  $\phi_{ZYX-rot}$  with  $z \in [-\theta, \theta]^3$  and  $\theta \in [0, \pi/2]$  belongs to the set of general rotations  $\phi_R$  with parameter space  $\mathcal{Z}_R = S^2 \times [0, 2\theta]$ .

### B.4. Proof of Theorem 3: Certifying Z-taper $\circ$ Z-rotation

*Proof.* Consider the composite transformation  $\phi_{TP} \circ \phi_{Rot-z}$  with parameter space  $\mathcal{Z} = \mathcal{Z}_{TP} \times \mathcal{Z}_{Rot-z} = \mathbb{R}^2$ . As stated in Theorem 3, we sample  $\varphi\theta M^2$  parameters  $z_{jk} = (\varphi_j, \theta_k)$  in the subspace  $S = [-\varphi, \varphi] \times [-\theta, \theta] \subseteq \mathcal{Z}$ , with  $\varphi_j = \frac{2j}{M} - \varphi$  and  $\theta_k = \frac{2k}{M} - \theta$ . The interpolation error of a point cloud  $x = \{p_i\}_{i=1}^N$  ( $p_i = x_i, y_i, z_i$ ) between two transformations  $z_{jk} = (\varphi_j, \theta_k)$  and  $z' = (\varphi', \theta')$  is:

$$\mathcal{M}(z_{jk}, z') = \left( \sum_{i=1}^N \|\phi_{TP}(\phi_{Rot-z}(p_i, \theta_k), \varphi_j) - \phi_{TP}(\phi_{Rot-z}(p_i, \theta'), \varphi')\|_2^2 \right)^{1/2} \quad (64)$$

$$= \left( \sum_{i=1}^N \|\phi_{TP}(p'_i, \varphi_j) - \phi_{TP}(\phi_{Rot-z}(p'_i, \theta' - \theta_k), \varphi')\|_2^2 \right)^{1/2} \quad \text{where } p'_i = \phi_{Rot-z}(p_i, \theta_k) \quad (65)$$

$$= \left( \sum_{i=1}^N \left[ (1 + \varphi_j z'_i)^2 r_i'^2 + (1 + \varphi' z'_i)^2 r_i'^2 - 2(1 + \varphi_j z'_i)(1 + \varphi' z'_i) r_i'^2 \cos(\theta' - \theta_k) \right] \right)^{1/2}, \quad (r_i'^2 = x_i'^2 + y_i'^2) \quad (66)$$

$$\leq \left( \sum_{i=1}^N \left[ (\varphi' - \varphi_j)^2 z_i'^2 r_i'^2 + (\theta' - \theta_k)^2 r_i'^2 (1 + \varphi_j z'_i)(1 + \varphi' z'_i) \right] \right)^{1/2} \quad (67)$$

Equation (66) uses the law of cosine to compute the  $\ell_2$  distance. Note that  $\max_{\theta'} \min_k |\theta' - \theta_k| = \frac{1}{M}$  and  $\max_{\varphi'} \min_j |\varphi' - \varphi_j| = \frac{1}{M}$ . Also,  $z_i'^2 r_i'^2 \leq \frac{1}{4}$  for  $z_i'^2 + r_i'^2 \leq 1$ . Therefore, the interpolation error

$$\mathcal{M}_S = \max_{z=(\varphi', \theta') \in S} \min_{j,k} \mathcal{M}(z_{jk}, z') \quad (68)$$

$$\leq \left( \sum_{i=1}^N \left( \frac{1}{4M^2} + \frac{(1+\varphi)^2}{M^2} \right) \right)^{1/2} \quad (69)$$

$$= \frac{\sqrt{N(4\varphi^2 + 8\varphi + 5)}}{2M} \quad (70)$$

It thus follows from Theorem 6 that for any  $z \in S$ ,  $y_A = \arg \max_y q(y|\phi(x, z); \epsilon)$ ; if  $\forall j, k$ :

$$\frac{\sigma}{2} \left( \Phi^{-1} \left( p_A^{(jk)} \right) - \Phi^{-1} \left( p_B^{(jk)} \right) \right) \geq \frac{\sqrt{N(4\varphi^2 + 8\varphi + 5)}}{2M}. \quad (71)$$

### B.5. Proof of Theorem 4: Certifying Z-twist $\circ$ Z-taper $\circ$ Z-rotation

*Proof.* The composite transformation  $\phi_{Tz} \circ \phi_{TP} \circ \phi_{Rot-z}$  has a parameter space of  $\mathcal{Z} = \mathcal{Z}_{Twist} \times \mathcal{Z}_{Taper} \times \mathcal{Z}_{Rot-z} = \mathbb{R}^3$ . We calculate the interpolation error of a point cloud  $x = \{p_i\}_{i=1}^N$  between two transformations  $z_{jkl} = (\varphi_j, \alpha_k, \theta_l)$  and  $z' = (\varphi', \alpha', \theta')$ . (Note that z-twist, z-taper and z-rotation are pairwise commutative.)

$$\mathcal{M}(z', z_{jkl}) = \|\phi(x, z_{jkl}) - \phi(x, z')\|_2 \quad (72)$$

$$= \left( \sum_{i=1}^N \|\phi(p_i, z_{jkl}) - \phi(p_i, z')\|_2^2 \right)^{1/2} \quad (73)$$

$$= \left( \sum_{i=1}^N \|\phi_{TP}(p'_i, \alpha_k) - \phi_{TP}(\phi_{Tz}(\phi_{Rot-z}(p'_i, \theta' - \theta_l), \varphi' - \varphi_j), \alpha')\|_2^2 \right)^{1/2} \quad (74)$$

$$= \left( \sum_{i=1}^N \left[ (1 + \alpha_k z'_i)^2 r_i'^2 + (1 + \alpha' z'_i)^2 r_i'^2 - 2(1 + \alpha_k z'_i)(1 + \alpha' z'_i) r_i'^2 \cos((\varphi' - \varphi_j) z'_i + \theta' - \theta_l) \right] \right)^{1/2} \quad (75)$$

$$\leq \left( \sum_{i=1}^N \left[ (\alpha_k - \alpha')^2 z_i'^2 r_i'^2 + (1 + \alpha_k z'_i)(1 + \alpha' z'_i) ((\varphi' - \varphi_j) z'_i + \theta' - \theta_l)^2 r_i'^2 \right] \right)^{1/2} \quad (76)$$

Equation (75) uses the law of cosine for computing the  $\ell_2$  distance. Following the sampling strategy, for  $z' = (\varphi', \alpha', \theta') \in S = [-\varphi, \varphi, -\alpha, \alpha, -\theta, \theta]$ , we have  $\max_{\varphi'} \min_j |\varphi' - \varphi_j| = \frac{1}{M}$ ,  $\max_{\alpha'} \min_k |\alpha' - \alpha_k| = \frac{1}{M}$  and  $\max_{\theta'} \min_l |\theta' - \theta_l| = \frac{1}{M}$ . Hence, the maximum interpolation error for the subspace  $S$  is

$$\mathcal{M}_S = \max_{z' \in S} \min_{j,k,l} \mathcal{M}(z', z_{jkl}) \quad (77)$$

$$\leq \left( \sum_{i=1}^N \left[ \frac{z_i'^2 r_i'^2}{M^2} + \frac{(1 + \alpha z'_i)^2 (1 + z'_i)^2 r_i'^2}{M^2} \right] \right)^{1/2} \quad (78)$$

$$\leq \left( \sum_{i=1}^N \left( \frac{1}{4M^2} + \frac{(1 + \alpha)^2 \times \frac{27}{16}}{M^2} \right) \right) = \frac{\sqrt{N(1 + \frac{27}{4}(1 + \alpha)^2)}}{2M} \quad (79)$$

Applying Theorem 6, it is guaranteed that for any  $z \in S$ ,  $y_A = \arg \max_y q(y|\phi(x, z); \epsilon)$ , if  $\forall j, k, l$ ,

$$\frac{\sigma}{2} \left( \Phi^{-1} \left( p_A^{(jkl)} \right) - \Phi^{-1} \left( p_B^{(jkl)} \right) \right) \geq \frac{\sqrt{N(1 + \frac{27}{4}(1 + \alpha)^2)}}{2M} \quad (80)$$

### C. Discussion on $\ell_p$ Norm Bounded Perturbations

We exhibit the certified robust accuracy under attacks with restricted  $\ell_p$  norm in Table 6. Our TPC framework is directly applicable for certifying  $\ell_2$  norm bounded attacks. We smooth a base classifier by additive noise  $\epsilon \sim \mathcal{N}(0, \mathbb{1}_{3 \times N})$  so its class probability is  $q(y|x; \epsilon) = \mathbb{E}_\epsilon p(y|x + \epsilon)$ . Since additive noise is an additive transformation, the smoothed classifier must be robust for any attacks  $\alpha \in \mathbb{R}^{3 \times N}$  with

$$\|\alpha\|_2 \leq \frac{\sigma}{2} \left( \Phi^{-1}(p_A) - \Phi^{-1}(p_B) \right). \quad (81)$$

Though our TPC framework cannot directly be applied to certify against  $\ell_\infty$  norm bounded perturbations, we can still derive a certification bound for point clouds  $x \in \mathbb{R}^{3 \times N}$  by a loose relaxation  $\|\theta\|_\infty \leq \sqrt{3N} \|\theta\|_2$ . However, this relaxation from  $\ell_2$  to  $\ell_\infty$  is too imprecise when applying it in a high dimensional space. As a result, the certified accuracy for  $\ell_\infty$  norm drops as the point cloud size increases.

Table 6. Certified robustness for point cloud models under different  $\ell_p$  attacks. We achieve similar certification bound for  $\ell_\infty$  norm bounded attack as DeepG3D (Lorenz et al., 2021)

Attack	Radius	TPC			DeepG3D	
		16	64	256	64	256
$\ell_2$	0.05	74.1	82.2	<b>84.2</b>	-	-
$\ell_2$	0.1	61.9	70.8	<b>77.3</b>	-	-
$\ell_\infty$	0.01	<b>70.9</b>	64.4	47.0	<b>70.9</b>	67.0

### D. Certified Ratio

Certified ratio is defined as the fraction of test point clouds classified *consistently*, but not necessarily *correctly* under a set of attacks. We compare the certified ratio achieved by our TPC method with the baseline, DeepG3D (Lorenz et al., 2021) in Table 7.

Table 7. Comparison of certified ratio achieved by our transformation specific smoothing framework TPC and the baseline, DeepG3D (Lorenz et al., 2021). “-” denotes the settings where the baselines cannot scale up to.

Transformation	Attack radius	Certified Ratio (%)	
		TPC	DeepG3D
ZYX-rotation	2°	<b>92.6</b>	72.8
	5°	<b>79.5</b>	58.7
General rotation	5°	<b>89.4</b>	-
	10°	<b>79.5</b>	-
	15°	<b>63.1</b>	-
Z-rotation	20°	<b>99.0</b>	96.7
	60°	<b>98.1</b>	95.7
	180°	<b>95.2</b>	-
Z-shear	0.03	<b>98.6</b>	70.7
	0.1	<b>97.1</b>	-
	0.2	<b>91.8</b>	-
Z-twist	20°	<b>83.8</b>	23.9
	60°	<b>80.1</b>	-
	180°	<b>64.3</b>	-
Z-taper	0.1	<b>95.2</b>	81.5
	0.2	<b>93.3</b>	28.3
	0.5	<b>91.2</b>	-
Z-twist ◦ Z-rotation	20°, 1°	<b>96.5</b>	16.3
	20°, 5°	<b>96.0</b>	-
Z-taper ◦ Z-rotation	50°, 5°	<b>95.0</b>	-
	0.1, 1°	<b>89.5</b>	68.5
Z-twist ◦ Z-taper ◦ Z-rotation	0.2, 1°	<b>86.1</b>	20.7
	10°, 0.1, 1°	<b>74.9</b>	20.7
	20°, 0.2, 1°	<b>68.7</b>	5.4